doi: 10.15407/ujpe60.07.0648

N.V. BONDAR,[1] M.S. BRODYN,[1] N.A. MATVEEVSKAYA[2]

[1] Institute of Physics, Nat. Acad. of Sci. of Ukraine
(46, Nauky Ave., Kyiv 03680, Ukraine; e-mail: jbond@iop.kiev.ua)
[2] Institute for Single Crystals, Nat. Acad. of Sci. of Ukraine
(60, Lenin Ave., Kharkiv, 61178, Ukraine)

QUANTUM-SIZE EFFECT AND EXCITON PERCOLATION IN POROUS AND DISORDERED FILMS ON THE BASIS OF SPHERICAL "CORE/SHELL" ELEMENTS

PACS 73.21 La, 78.55 Ft

The results of spectroscopic researches of porous and disordered films fabricated on the basis of spherical elements of the "core/shell" type, SiO_2/CdS nanoparticles (SiO_2 spheres covered with CdS quantum dots) are reported. The quantum-size effect of excitons in the quantum dots located on the surface of spheres is found to depend on the sphere size and to weakly depend on the quantum dot radius, which results from the quantization of the exciton motion normally to the sphere surface. The quantization survives, even if the sphere coverage exceeds the exciton percolation threshold. To evaluate the latter in the film plane and to determine the critical concentration of SiO_2/CdS nanoparticles, a number of specimens on the basis of the mixtures 20–80% SiO_2 : 80–20% SiO_2/CdS are studied. The exciton percolation threshold is registered in those structures for the first time at a fraction of SiO_2/CdS nanoparticles in the mixture of about 60%, which is twice as high as the value predicted by the hard sphere model. A qualitative explanation of this phenomenon is proposed.

Keywords: exciton, quantum-size effect, exciton percolation, quantum dot.

1. Introduction

The most important feature of semiconductor quantum dots (QDs) is the dependences of the energies of excited electrons and holes in those dots on their size, the so-called quantum-size effect. Nowadays, it is considered to be well studied in the case of QDs with relatively simple shapes (spherical, cubic, trapezoidal, *etc.*) grown up in dielectric or polymer matrices [1]. Therefore, the main attention is concentrated on the research of more complicated structures of the type "core/shell", in which the core is a QD with the spherical, hexagonal, cluster, or any other form, whereas the shell is always a sphere [1]. The shell is a semiconductor with the energy gap width larger than that in the QD. It plays two roles: it passivates the dangling bonds of external atoms in the QD and serves as a potential barrier for electrons and holes. This form of the structure allows the quantum yield to be considerably enhanced owing to the damping of Auger processes by increasing their relaxation time, in comparison with the emission ones, by modifying the shape of interface between two phases [2]. Such structures make it possible to calculate the energy of $1S$ state of excitons more precisely and to compare it with experimental data, because the depths of the corresponding potential wells in the core and the shell can be easily evaluated, and the values of their material parameters are well-known. They are promising objects serving as a basis for biomarkers, active elements of light-emitting diodes (LED), lasers, single photon sources for quantum information processes, and elements of solar cells [1].

The mentioned structures, owing to their quick commercial application, are intensively studied. However, there exists another group of structures of the "core/shell" type, which have been investigated much less at present. Their core is not a quantum object, but plays the role of a substrate, whereas the shell is composed of QDs made of II–VI semiconductors located on its surface.

In this work, we report the results of researches of such structures. Spheres of silicon dioxide (SiO_2) play the role of the core. Their surface is covered to vari-

ous coverage degrees with CdS QDs of various radii. The exciton size effect in those systems was demonstrated to have its specificity in the dependence on the QD radius. The effect is observed even if the QD radius is twice as large as the corresponding Bohr radius. Films obtained on quartz substrates from a mixture of pure SiO_2 spheres and SiO_2 spheres covered with CdS QDs (SiO_2/CdS; below referred to as nanoparticles, NPs) are analyzed. Those systems may probably be the only microscopic systems with continual percolation, where the critical concentration of NPs at the exciton percolation threshold can be calculated and compared with the experimental value. The percolation threshold in those systems is found to arise at a concentration of SiO_2/CdS nanoparticles in the mixture of about 60%, which is twice as high as the value predicted by the so-called hard sphere model [3]. A qualitative explanation of this fact is proposed.

2. Experimental Results

Monodisperse SiO_2 spheres with the diameter $D \approx$ $\approx$ 300 nm and a size dispersion of less than 7% were fabricated using a modified Stober method [4]: hydrolysis of tetraethyl orthosilicate followed by condensation in the absolute ethanol medium. SiO_2 spheres were synthesized at the temperature $T = 30$ °C provided the molar ratio of reagents $TEOC : NH_4OH : H_2O = 1 : 12.5 : 47$. CdS QDs were obtained by performing the exchange reaction in aqueous solutions in the presence of a stabilizer (polyacrylic acid, PAA) with $M_w = 2000$ g/mol and a concentration of 0.07 wt.%:

$$CdCl_2 + Na_2S = CdS \downarrow + 2NaCl.$$

Macromolecules of the PAA stabilizer form a protective shell on the CdS QD surface, which prevents the aggregation of QDs. The application of PAA as a stabilizer gave rise to the formation of QDs with the radius $R_0 \approx 2$ nm, and the application of polyvinylpyrrolidone and gelatin macromolecules to the formation of QDs with the radius $R_0 \approx 7$ and 13 nm, respectively; in all cases, QDs had a spherical form. The average radius of CdS QDs was calculated by data of the transmission electron microscopy. The electron diffraction patterns testify to the crystalline structure of CdS QDs with the cubic symmetry of their crystal lattice. The corresponding histogram of the CdS QD distribution over sizes shows a high uniformity of QD dimensions (Fig. 1).

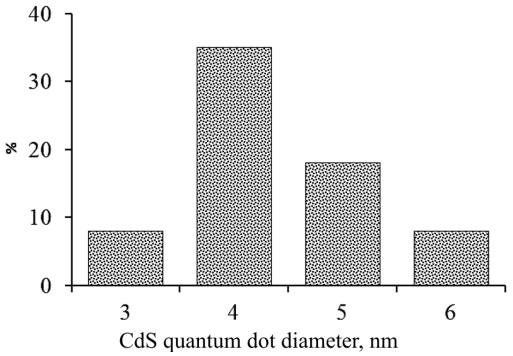

Fig. 1. Histogram of the distribution of CdS QDs over their size

In the course of NP formation, the adsorption of CdS QDs on the surface of SiO_2 spheres has to be controlled. First, a buffer layer with ordered functional groups for the electrostatic binding of CdS QDs with the template surface has to be formed. The modification of the SiO_2 surface by a monolayer of bifunctional organic molecules provides a recharge of the surface and reduces its high surface energy. The formation of a monolayer of modifying organic molecules on the surface of the spheres prevents from the undesirable interaction of functional groups with one another and excludes the appearance of steric obstacles for a uniform arrangement of QDs over the template surface. As a modifying compound, 3-aminopropyltriethoxysilane, $H_2N(CH_2)_3Si(OC_2H_5)_3$, was chosen. Its molecules form a covalent chemical bond with silanol groups on the SiO_2 surface and, due to the presence of an amino group, provide the adsorption of CdS QDs on the sphere surface.

Templates consisting of SiO_2 spheres demonstrate a feature in the dependence of the activity of silanol groups located on the sphere surface on the surface curvature; namely, as the radius diminishes, the number of groups on the surface grows. Hence, if the surface of nanotemplates is modified, the largest number of active centers are formed on the surface of SiO_2 spheres with a small diameter. However, as the diameter of SiO_2 spheres decreases below $D \approx 100$ nm, the degree of their aggregation in the solution grows as a result of the surface energy excess growth. Therefore, in this work, SiO_2 spheres with $D \approx 300$ nm were used. SiO_2/CdS nanoparticles were obtained using the method of controllable adsorption of isolated CdS

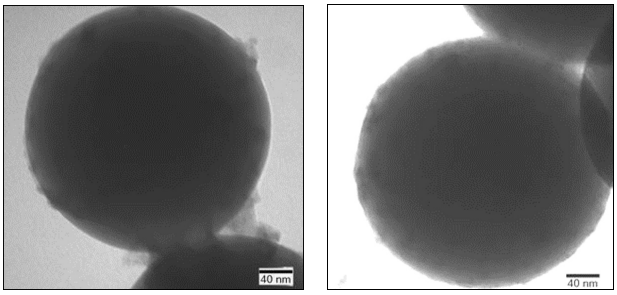

a *b*

Fig. 2. TEM images of SiO_2/CdS nanoparticles with various degrees of filling of a sphere with CdS QDs with $R_0 \approx 2$ nm: 20 (*a*) and 50% (*b*)

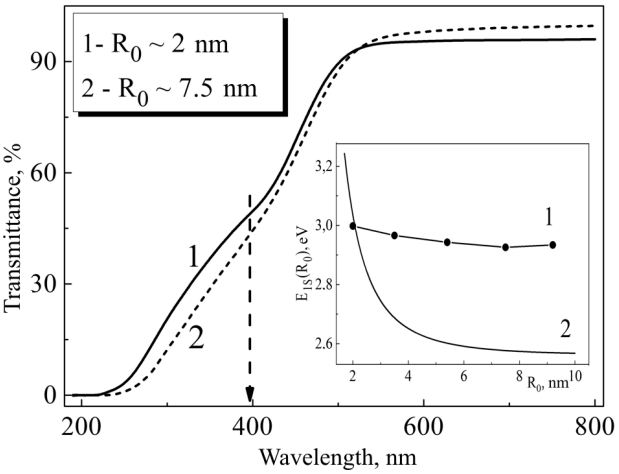

Fig. 3. Absorption spectra of two specimens with CdS QDs with $R_0 \approx 2$ (*1*) and 7.5 nm (*2*). In the inset: (*1*) the energy of the exciton $1S$ state in specimens with $R_0 \approx 2$ and 7.5 nm; (*2*) the dependence $E_{1S}(R_0)$ (Eq. (2)), $E_{g0} = 2.54$ eV is the energy gap width in the bulk CdS

QDs from an aqueous solution onto the surface of SiO_2 spheres at the temperature $T = 20 \pm 2$ °C. The elevation of the synthesis temperature gave rise to a reduction of the aggregation resistance of the obtained suspensions of SiO_2/CdS nanoparticles, and their adhesion and coagulation.

To provide a uniform coverage of the SiO_2 sphere surface with CdS QDs and to prevent the formation of conglomerates on their surface, the adsorption process was carried out under the condition of QD deficiency. It was established experimentally that, within one 2-hour cycle of adsorption, about 15% of the SiO_2 sphere surface became filled. To increase the filling concentration, the adsorption cycles were repeated until a surface filling of about 50% was reached. In Fig. 2, the microphotos of NPs with different degrees of surface filling are shown. The filling degree was estimated as the ratio between the area of the sphere surface filled with QDs and its total surface area. In the course of adsorption, CdS QDs were regularly distributed over the SiO_2 surface to form a monolayer with a thickness determined by R_0. The obtained SiO_2/CdS nanoparticles did not agglomerate. They had a spherical shape and a narrow distribution over sizes. In the first group of films 6–8 μm in thickness and fabricated on the basis of only SiO_2/CdS nanoparticles, the surface of the spheres was filled with QDs to about 20% in order to prevent the interaction between QDs with $R_0 \approx 2 \div 9.6$ nm.

The second group of films with the same thickness was obtained on the basis of a mixture of pure SiO_2 spheres and SiO_2/CdS nanoparticles with a degree of filling of the SiO_2 surface with CdS QDs of about 50% and $R_0 \approx 2$ nm. The ratio $SiO_2 : (SiO_2/CdS)$ in the mixture was 20 : 80, 30 : 70, 50 : 50, 60 : 40, and 80 : 20. The films were fabricated by spraying the NP suspension with the given concentration on a heated glass substrate. To improve the adsorption of the first NP layer, substrates were modified by 3-aminopropyltriethoxysilane molecules. As a film-forming agent, polyacrylic acid $[–CH_2CH(COOH)–]_n$ with a molecular mass of 100000 g/mol was used. The mass of films was monitored using the gravimetric technique. For all specimens, it was kept constant within the interval of about 0.004–0.005 g

The films under study were porous and had a disordered structure. Therefore, they were characterized by a substantial light scattering, which resulted in the smearing of peaks in the absorption (AS) or transmission (TS) spectra. As a result, it was rather difficult to determine the exciton $1S$ transition energy. In Fig. 3, only two TS curves for the films from the first group (specimens with $R_0 \approx 2$ and 7.5 nm) are shown as an evidence. The both curves demonstrate a feature in a vicinity of about 400 nm (it is marked by an arrow), which is associated with the $1S$ exciton state in the CdS QDs. However, it is impossible to determine the state energy more accurately. Therefore, those specimens were used to register the diffuse reflection spectra (DRS). The latter were analyzed in the framework of the Kubelka–Munk model, $F(R) = (1-R)^n/2R$, from whence the forbidden gap edge in the specimen with the corresponding R_0 was determined (Fig. 4).

The absorption and photoluminescence (PL) spectra for the specimens of the second group are depicted in Fig. 5. One can see that the AS curve also has an inflection point at about 400 nm, but it is also hard to precisely determine the energy position of the exciton $1S$ state in CdS QDs. The DRSs registered for these films coincided with their analogs for the films from the first group with $R_0 \approx 2$ nm; therefore, curve *1* in Fig. 4 is common for the specimens from both groups.

The size, morphology, and element composition of synthesized specimens were studied with the help of a transmission electron microscope PEM-125 with an accelerating voltage of 100 kV, and a scanning electron microscope JSM-6390 LV with an energy dispersive spectrometer INCA Energy 350 and an electron backscattered diffraction detector NKL Channel-5 EBSD. The specimens were fabricated following a standard technique consisting in depositing the colloid solutions of specimens on copper films covered with a thin carbon layer or on nickel substrates, with the subsequent drying at room temperature. The chemical structure of specimens was analyzed with the help of a spectrophotometer XPS-800 Kratos. Photoelectrons were excited using MgK_α radiation ($h\gamma = 1253.6$ eV), and their kinetic energy was determined with the help of a hemispherical electrostatic analyzer. Specimens for researches were deposited on the titanium substrate surface; the thickness of analyzed layers was about 5 nm. The optical TS, AS, and DRS were registered with the help of a spectrometer SPEKORD M40, and the PL spectra were obtained, by using a spectral installation with a resolution not worse than 0.5 nm at room temperature. The excitation was performed using a He–Cd laser with the wavelength $\lambda_{ex.} = 325$ nm and a power of about 10 mW.

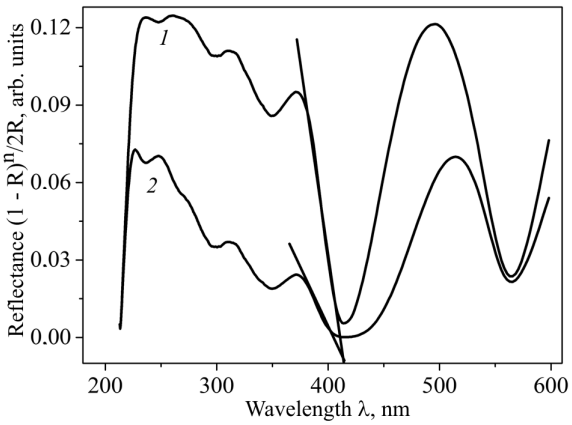

Fig. 4. Spectra of diffusive reflection for films with $R_0 \approx 2$ (*1*) and 7.5 nm (*2*) recalculated according to the Kubelka–Munk model with $n = 1$

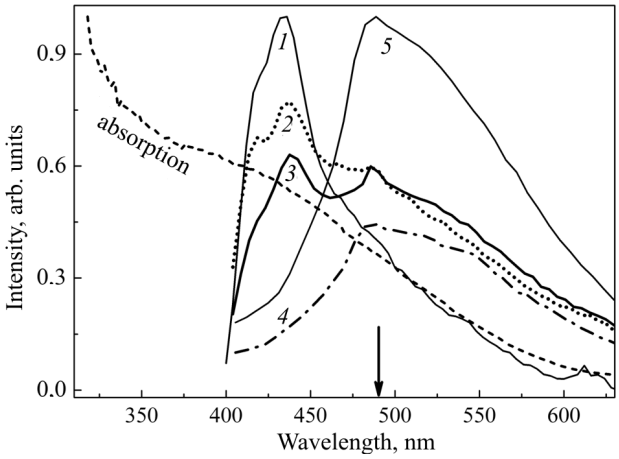

Fig. 5. Absorption and PL spectra of the second-group specimens with various ratios $SiO_2 : (SiO_2/CdS)$: 80 : 20 (*1*), 70 : 30 (*2*), 50 : 50 (*3*), 40 : 60 (*4*), and 20 : 80 (*5*). The arrow marks the position of the forbidden gap in the bulk CsS (about 488 nm)

3. Discussion of Results

3.1. Exciton size effect feature in sparse arrays of quantum dots on a spherical surface

Before proceeding to the analysis of the results obtained, let us consider some features in the covering of a sphere surface with symmetric objects equal by their dimensions, e.g., spherical circles (caps). This analysis is necessary, first, to substantiate the coating magnitude of SiO_2 spheres with CdS QDs and determine a regime, in which the exciton system exists on the sphere surface. Second, such an analysis has never been carried out earlier for those and similar structures, which are mainly synthesized by chemists [5–12].

Let us consider a circle with the spherical (angular) radius R_0 on the surface of a sphere with the radius R; the area of the circle equals $S_0 = 2\pi R^2[1 - \cos(R_0)]$. We have to determine the number of identical circles (in our case, these are CdS QDs) that can be arranged on the SiO_2 sphere in such a way that they would cover its surface as much as possible without mutual overlapping. At present, the problem has no complete mathematical solu-

tion. However, the limiting coating value in the case $N \to \infty$ is known [13],

$$\Sigma S_0 = N\frac{R^2}{2}\left[\frac{1}{2}\sin^{-1}\left(\frac{N}{N-2}\,\frac{\pi}{6}\right) - \cos(R_0)\right] < \\ < \sqrt{3}\,\frac{\pi}{6} \approx 0.907, \quad (1)$$

which equals about 74%, i.e. less than in the case of a plane surface (about 91%). Now, according to the obtained estimate, some conclusions can be drawn. In the examined films, the coverage areas of SiO_2 spheres with CdS QDs amount to 20 and 50%, which is smaller than the limiting value. Therefore, we may consider that, in the specimens with the 20%-covered surface, the excitons excited in the QDs preserve their individuality and do not interact with neighbor QDs, with the exciton system on the sphere surfaces remaining well below the percolation threshold. However, in the case where the coverage of the sphere surface is about 50%, the overlapping of the exciton wave functions at neighbor QDs becomes substantial, a percolation channel emerges, and the percolation threshold is overcome.

It has to be noted that, if the exciton size effect is preserved, it is rather difficult to determine the exact moment of percolation threshold formation in an array of QDs and their critical concentration (or the coverage degree of the surface area). It can be done more easily in 3D structures with QDs, where the formation of this threshold was registered in PL spectra [14]. As a rule, the percolation manifests itself in the disappearance of the exciton size effect and a change to the radiation emission of the system from the bulk phase. However, in our specimens, those phenomena were not observed. Therefore, under stationary excitation conditions, this transition can be detected by a reduction of the PL band intensity at the percolation threshold. But, for this purpose, it is necessary to precisely monitor the number of CdS QDs on the sphere surface of various specimens, which is hard to perform in the framework of the available technology. Therefore, the temporal measurements of the exciton radiative recombination damping in specimens with various coverage degrees of the SiO_2 sphere surface are required.

Now, let us analyze the exciton quantum-size effect in sparse arrays of CdS QDs that cover about 20% of the SiO_2 sphere surface. Curve *1* in the inset of Fig. 3 exhibits the experimental dependence $E_{1S}(R_0)$ of the exciton $1S$ state energy obtained for the specimens from the first group. It is evident that, although the dependence is shifted with respect to the energy gap in the bulk CdS ($E_{g0} \approx 2.54$ eV) toward blue wavelengths as a result of the exciton motion quantization, it is almost independent of R_0. In order to explain this fact, let us consider the exciton size effect, which now is a well-studied phenomenon. Provided the correspondence between the dielectric constants of QDs and the matrix, the solution of the Schrödinger equation obtained in the framework of the one-band model determines the following exciton $1S$ state energy in a spherical QD [1]:

$$E_{1S}(R_0) = E_{g0} + \frac{\pi^2\hbar^2}{2\mu R_0^2} - 1.786\frac{e^2}{\varepsilon_0 R_0} - 0.248\varepsilon_x, \quad (2)$$

where μ is the reduced exciton mass, and $\varepsilon_x \approx 28$ meV and $\varepsilon_0 = 8.7$ are the binding energy in and the dielectric constant of the crystalline CdS, respectively. The dependence $E_{1S}(R_0)$ is plotted in the inset of Fig. 3 (curve *2*). It should be noted that this solution for CdS QDs on the sphere surface is approximate, because of the QDs contact with different media: on the one side, this is the SiO_2 sphere and, on the other side, the PAA stabilizer film covering the QD surface. As a result, there emerges an asymmetric potential well for electrons and holes in a CdS QD. It is difficult to estimate its depth, because the discontinuities of the valence and conduction bands at the interface between two phases – the indicated media and the QD – are not known even approximately. Nevertheless, let us use Eq. (2) to approximately estimate $E_{1S}(R_0)$ by assuming the potential well for excitons to be infinitely deep.

In the specimens belonging to the first group, the $E_{1S}(R_0)$ values almost coincide for the specimens with $R_0 \approx 2$ and 7.5 nm, being equal to the value given by Eq. (2) at $R_0 \approx 2$ nm. As R_0 increases further, the experimental $E_{1S}(R_0)$ values start to substantially deviate from the calculated ones, and the exciton size effect in CdS QDs on the sphere surface does not depend anymore on R_0. Nevertheless, the size effect survives, even if R_0 considerably exceeds the Bohr radius of excitons in the bulk CdS. Evidently, this is a result of the high surface energy of SiO_2 spheres. Although its magnitude is reduced owing to the recharge by organic molecules, but it remains sufficient to distort the QD shape, which was initially spherical, but became disk- or lens-like under its ac-

tion [15]. The height of a quantum disk or lens on the sphere surface increases a little as R_0 grows, and, as a result, the energy of excitons in this disk decreases, as one can see from the experimental curve in the inset of Fig. 3. In spite of that, rather a strong exciton size effect survives in the QD in the direction normal to the sphere surface. This is why the exciton size effect depends weakly on the radius R_0 of CdS QDs located on the sphere surface. However, it is known that the surface energy of the spheres depends on their characteristic dimension R_0, which determines their volume and the number of molecules in them. Therefore, the exciton size effect in QDs would more likely depend on the radius R of SiO_2 spheres, i.e. the substrate dimensions, than on R_0. This is a feature that distinguishes the systems concerned among the others. Further researches of those objects will allow this dependence to be determined more precisely and an expression relating $E_{1S}(R_0)$ and the dimensions of spherical templates, on which QDs are grown, to be obtained.

3.2. Formation of the exciton percolation level in the films of mixtures of pure SiO_2 spheres and SiO_2/CdS nanoparticles

When studying similar structures with ZnO QDs, we came to a conclusion that, in those systems, there exist two consecutive phase thresholds of exciton percolation: on the surface of the spheres and in the plane of the films synthesized from those objects [16]. If the film is formed from SiO_2/CdS nanoparticles only, the emergence of the percolation threshold on the surface of SiO_2 spheres, provided its critical coverage with CdS QDs, will automatically bring about the smearing of the exciton wave function in the film plane as well. However, if the coverage of the sphere surface is not enough, as it occurs in the films belonging to the first group (about 20%), the percolation threshold will not arise in them, in spite of the fact that they were synthesized from NPs only. In the specimens of the second group with a coverage of about 50%, the number of CdS QDs is sufficient for the threshold to be formed on the sphere surface. The emergence of the second exciton threshold depends on the concentrations of NPs and pure SiO_2 spheres in the films, which will be discussed below.

The analyzed structure, i.e. the mixture of NPs and pure SiO_2 spheres, is classed to the so-called "color percolation" models [17]. For an explanation, let us consider a volume filled with hard spheres (a random dense packing), some of which (nonconducting) are painted white, whereas the others (conducting) are black. Let us determine the critical concentration of black spheres, at which the whole system is conducting. The fraction of black, or conducting, spheres in this mixture is known to equal 25–30% at the percolation threshold [3]. Assuming pure SiO_2 spheres to be nonconducting and SiO_2/CdS nanoparticles conducting, it is possible to experimentally determine the fraction of the latter at the percolation threshold and to compare the result with that predicted by the model of color spheres.

In Fig. 5, the absorption spectrum discussed above and the PL band for the films of the second group with a coverage of about 50% and the corresponding concentrations of pure SiO_2 and NPs are depicted. The PL band of specimens with a low NP fraction (about 20%) is shifted toward the blue side of the spectrum by approximately 420 meV owing to the exciton size effect in QDs. It consists of two peaks separated by about 120 meV. The maximum of the short-wave peak coincides with $E_{1S}(R_0)$ determined from curve *1* in Fig. 4. The origin of the splitting is not known, but a similar splitting by about 160 meV was revealed by us in 3D specimens of CdS QDs grown up in borosilicate glass, and the corresponding explanation of its nature was given [18].

Now, let us analyze the dependence of the PL band in Fig. 5 on the NP concentration in the mixture. If the NP number is small (20%), curve *1* is rather narrow and asymmetric with a broad long-wave tail. The nature of the states in this tail is most likely related to PAA molecules and Si=O bonds on the surface. As the NP fraction in the mixture increases, the intensities of short-wave peaks in the PL band decrease. Instead, on its long-wave wing, there emerges a pronounced peak with a maximum coinciding with the edge of the forbidden gap in the bulk CdS, E_{g0}, curves *2* and *3*. If the NP concentration in the mixture exceeds 50%, both short-wave peaks in the PL band disappear almost completely, whereas the wide asymmetric peak at about E_{g0} quickly grows with the NP concentration. Such a behavior of the PL band testifies that, in the interval of NP concentrations near 60%, there emerges an exciton percolation level in the films, which is accompanied by an almost total disappearance of the exciton size effect. Here is a brief substantiation of this phenomenon.

If the NP concentration in the mixture is low, the majority of NPs are isolated, being surrounded by pure SiO_2 spheres. As the NP concentration increases, finite-size NP clusters composed of 2, 3, 4, ... NPs start to form, in which, owing to their dimensions, the exciton size effect disappears. Due to the exciton recombination in such clusters, the energy of photons falls within the interval of E_{g0}, and they give no contribution to short-wave PL peaks. Hence, the intensity of the latter starts to diminish as the NP concentration increases (curves *2* and *3*). Finally, when the NP concentration in the mixture reaches about 60%, a percolation cluster of excitons appears due to the smearing of exciton wave functions over a macroscopic distance. As a result, the quantum-size effect and the short-wave peaks in the PL band disappear (curve *4*). A further growth of the NP concentration in the mixture gives rise to the growth of the PL intensity as a consequence of the simple increase of the QD number in the system. The hard-sphere model mentioned above can cast light on the formation of the exciton percolation level in the system concerned. At a random dense packing, every black sphere is surrounded by 12 other spheres; this is its coordination number. For a global connectivity over the black spheres to arise in the system, it is necessary that, among those 12 spheres, about 2.8 ones have to be black [3]. The applied technology makes our films porous, so that they considerably deviate from the dense packing model in that the coordination number of every nanoparticle in the mixture is evidently smaller than 12. Therefore, in order that the exciton percolation threshold over the NPs emerge, a higher NP concentration in the mixture than that predicted by the hard-sphere model is required. That is why the percolation transition in our systems is observed at the NP concentration (about 60%) that is almost twice as high as that predicted by the hard-sphere model. For a quantitative explanation of this phenomenon, the number of contacts for every NP at the percolation threshold, the number of CdS QDs in those contacts, and other features of the systems concerned have to be taken into account, which will be done elsewhere.

To summarize, the features of the exciton size effect in semiconductor QDs located in a topologic space different from 3D and 2D ones – namely, on the surface of spherical objects – were revealed in this work. It is shown for the first time that the ordinary dependence of the exciton energy on the QD radius is transformed into the dependence on the dimensions of the substrate, on which the QDs were grown up, i.e. on the dimensions of spherical templates. All that is a result of the high surface energy of spheres, which deforms the QDs so that the exciton energy is quantized only in the direction normal to the surface. Another result is also obtained for the first time: namely, the exciton percolation level is revealed in films fabricated from the mixture of pure SiO_2 spheres and SiO_2/CdS nanoparticles taken in the ratio that is twice as high as that predicted by the model of "color percolation" or the hard-sphere one. This result follows from a porous disordered structure of the films fabricated on the basis of spherical objects and from a reduction in the number of NP contacts in comparison with the random dense packing of hard spheres.

The work was carried out in the framework of the target-oriented complex program of findamental researches of the NAS of Ukraine "Fundamental problems of nanostructure systems, nanomaterials, nanotechnologies" (project NANO 14-10-N).

1. R.G. Chaudhuri and S. Paria, Chem. Rev. **112**, 2373 (2012).
2. G.E. Cragg and A.L. Efros, Nano Lett. **10**, 313 (2010).
3. S. Zallen, *The Physics of Amorphous Solids* (Wiley-VCH, Weinheim, 2004).
4. W. Stober and A. Fink, J. Coll. Interface Sci. **26**, 62 (1968).
5. N. Arul Dhas, A. Zaban, and A. Gedanken, Chem. Matt. **11**, 806 (1999).
6. A.L. Rogach, D. Nagesha, J.W. Ostrander, M. Giersig, and N.A. Kotov, Chem. Matt. **12**, 2676 (2000).
7. O.C. Monteiro, A. Catarina, C. Esteves, and T. Trindade, Chem. Matt. **14**, 2900 (2002).
8. M. Darbandi, R. Thomann, and T. Nann, Chem. Matt. **17**, 5720 (2005).
9. J. Yu, W. Liu, and H. Yu, Cryst. Growth Design **8**, 930 (2008).
10. T. Aubert, S.J. Soenen, D. Wassmuth, M. Cirillo, R. van Deun, K. Braeckmans, and Z. Hens, ASC Appl. Matt. Interfaces **6**, 11714 (2014).
11. Ch. Song-yuan, L. Liu, and S.A. Asher, J. Am. Chem. Soc. **116**, 6739 (1994).
12. Y. Fang, W.S. Loc, W. Lu, and J. Fang, Langmuir **27**, 14091 (2011).
13. T.W. Melnyk, O. Knop, and W.R. Smith, Can. J. Chem. **55**, 1745 (1977).
14. N.V. Bondar and M.S. Brodyn, Semiconductors **46**, 625 (2012).
15. S. Le Goff and B. Stebe, Phys. Rev. B **47**, 1383 (1993).
16. N.V. Bondar, M.S. Brodyn, Yu.V. Yermolayeva, and A.V. Tolmachev, Physica E **43**, 1882 (2011).

17. S.A. Ioselevich and A.A. Kornyshev, Phys. Rev. E **65**, 021301 (2002).
18. N.V. Bondar, J. Luminesc. **130**, 1 (2010).

Received 2013.
Translated from Ukrainian by O.I. Voitenko

М.В. Бондар, М.С. Бродин, Н.А. Матвєєвська

КВАНТОВО-РОЗМІРНИЙ ЕФЕКТ ТА ПЕРКОЛЯЦІЯ ЕКСИТОНІВ У ПОРУВАТИХ І НЕУПОРЯДКОВАНИХ ПЛІВКАХ НА ОСНОВІ СФЕРИЧНИХ ЕЛЕМЕНТІВ ТИПУ "ЯДРО/ОБОЛОНКА"

Р е з ю м е

У роботі наведено результати спектроскопічних досліджень поруватих та неупорядкованих плівок на основі сферичних елементів типу "ядро/болонка" – наночастинок SiO_2/CdS (сфери SiO_2 вкриті квантовими точками CdS). Виявлено, що квантово-розмірний ефект екситонів у квантових точках на поверхні сфер залежить від розміру останніх і слабо від радіуса квантових точок. Це є наслідком того, що квантування руху екситонів відбувається у напрямку, нормальному до поверхні сфери, зберігаючись навіть при величині її покриття, вище рівня протікання екситонів. З метою встановлення перколяційного порога екситонів у площині плівок та визначення критичної концентрації наночастинок SiO_2/CdS, було досліджено ряд зразків на основі сумішей $[SiO_2(20–80)\% : SiO_2/CdS(80–20)\%]$. Вперше у цих структурах зафіксовано поріг протікання екситонів при кількості наночастинок SiO_2/CdS у суміші $\sim 60\%$, що вдвічі перевищує величину, яку дає модель твердих сфер. Наведено якісне обґрунтування цього явища.